Direct Detection of Domains in Phospholipid Bilayers by Grazing Incidence Diffraction of Neutrons and Atomic Force Microscopy

C. Gliss,* H. Clausen-Schaumann,# R. Günther,§¶ S. Odenbach,§ O. Randl,¶ and T.M. Bayerl*
*Institut für Physik EP-5, Universität Würzburg, D-97074 Würzburg, Germany; #Lehrstuhl für Angewandte Physik, LMU-München, D-8799 Germany; §Institut für Materialwissenschaften, Bergische Universität GH Wuppertal, D-42285 Wuppertal, Germany; and ¶Institut Laue-Langevin, B.P. 156 X, F-38042 Grenoble Cedex, France

ABSTRACT The geometry of domains in phospholipid bilayers of binary (1:1) mixtures of synthetic lecithins with a difference in chain length of four methylene groups has been studied by two independent, direct and complementary methods. Grazing incidence diffraction of neutrons provided gel domain sizes of less than 10 nm in both the gel and the coexistence phase of the mixture, while no domains were detected for the fluid phase. For the coexistence region, the neutron data suggest that domains grow in number rather than in size with decreasing temperature. Atomic force microscopy was used to study gel phase size and shape of the domains. The domains imaged by atomic force microscopy exhibit a rather irregular shape with an average size of 10 nm, thus confirming the neutron results for this phase. The good agreement between atomic force microscopy and neutron results, despite the completely different nature of their observables, has potential for the future development of refined models for the interpretation of neutron data from heterogeneous membranes in terms of regularly spaced and spatially extended scatterers.

INTRODUCTION

Natural membranes consist essentially of proteins and lipids. Their unique bilayer structure serves as a matrix for proteins and is made up of a wide variety of lipids that differ significantly in size and structure. Understanding the physical properties of membranes such as their dynamics and micromechanics requires knowledge about the interaction between different lipids within the bilayer at a molecular scale. Microcalorimetric studies of model membranes consisting solely of lipids have shown that the thermodynamics of their mixing can be well described by regular solution theory (Lee, 1977; Lee, 1978). Together with computer simulations (Mouritsen, 1991; Pedersen et al., 1996), this suggests that clusters (domains) of lipids of the same kind form in the bilayer under conditions that may be relevant for biological systems.

Domains in lipid monolayers have been extensively studied experimentally with optical methods (Lösche et al., 1983; McConnell, 1991; McConnell et al., 1984; Möhwald, 1990). Recently, a micropartitioning of supported lipid bilayers into micrometer size mobile and immobile regions, induced by a litographically patterned solid support, was demonstrated by epifluorescence techniques (Groves et al., 1997). However, all attempts to visualize domains in biologically more relevant bilayers by optical methods have failed; consistently, a few studies using indirect methods have suggested a range of domain sizes below the optical limits (Almeida et al., 1992; Dolainsky et al., 1997; Mendelsohn et al., 1995; Sankaram et al., 1992). Even the presence of such tiny domains in natural membranes may have significant consequences for their macroscopic and microscopic properties (Loidl-Stahlhofen et al., 1996; Tate et al., 1991) as well as for the function of membranes (Knoll et al., 1991). Thus, new methods are required in order to determine geometry and distribution of domains in bilayers. Here, we describe a new experimental approach that provides the most direct measurement so far of domains in bilayers. It is based on the application of coherent scattering of evanescent neutrons together with atomic force microscopy (AFM).

We selected binary phospholipid mixtures that are well characterized by previous work (Jorgensen et al., 1993; Knoll et al., 1981b; Knoll et al., 1983) and that belong to a class of phospholipids (the lecithins) that are abundant in many natural membranes. An equimolar mixture of dimyristoyl phosphatidylcholine (DMPC) and distearoyl phosphatidylcholine (DSPC-d83) was used for neutron scattering in which the DSPC-d83 was perdeuterated except for the five protons on the glycerol backbone. Dipalmitoylphosphatidylcholine (DPPC) and diarachinoyl phosphatidylcholine (DAPC) were used for AFM experiments. In both mixtures, the length difference between the two lecithins caused by the different acyl chains is about 5 Å. This causes nonideal mixing leading to domain formation for the gel-fluid coexistence region and below the solidus line of the phase diagram (Knoll et al., 1981b; Lee, 1977; Mouritsen, 1991).

In-plane scattering of neutrons has not been previously used for the study of bilayer domain structures, the only biophysical application of this technique published so far having involved the determination of lateral distances between pore-forming proteins (He et al., 1996). In order to

Received for publication 2 December 1997 and in final form 21 January 1998.

Address reprint requests to Professor Thomas M. Bayerl, Universität Würzburg, Physikalisches Institut EP-5, D-97074 Würzburg, Germany. Tel. 49-931-888-5863; Fax: 49-931-888-5851; E-mail: tbayerl@physik.tu-muenchen.de.

0006-3495/98/05/2443/08 $2.00

validate the neutron approach for domain studies, we have also investigated domain structure in the gel phase using AFM, which has evolved as the most direct technique for studying the structure of biological surfaces on a molecular scale (Shao and Yang, 1995).

The combination of both methods is particularly interesting because they give complementary information. Although neutron scattering measurements are most directly represented in reciprocal space and involve contributions from a large number of domains, the AFM provides real space data and yields the geometry of single or comparatively few domains. An additional significant difference is that the AFM tip is in direct mechanical contact with the sample, thereby exerting loading forces in the range of several hundred piconewtons. This reduces the usefulness of AFM in the study of ultrasoft surfaces. Although it is possible to reduce the lateral forces acting on the sample significantly by using a dynamic imaging mode (Hansma et al., 1994), the remaining vertical forces are still comparable with the loading forces in contact mode (Radmacher et al., 1994). Therefore, the measured height can be influenced by the mechanical properties of the sample (Dufrêne et al., 1997; Rädler et al., 1994). This complicates the interpretation of AFM data obtained from ultrasoft samples like lipid membranes in the fluid phase. For this reason, we have restricted our AFM experiments to the mechanically stable gel phase while neutron experiments were performed additionally in the coexistence and fluid phase of the bilayer.

MATERIALS AND METHODS

Lipids

The following phospholipids were used: DMPC, DSPC-d83, DPPC, and DAPC. All lipids were purchased from Avanti Polar Lipids (Alabaster, AL). Highly purified water (≈18 MΩ/cm) was purchased from Milli-Q-Systems (Molsheim, France), and D_2O was from Sigma. Lipid mixtures were dissolved in chloroform to achieve thorough mixing. The chloroform was evaporated under nitrogen, and the mixture was then dried in a vacuum overnight. Afterwards, the lipids were rehydrated in purified water.

Differential scanning calorimetry

The phase diagram of DPPC/DAPC was measured using a Microcal MC-2 differential scanning calorimeter (Northampton, MA) at a scan rate of 30°C/h. The last two of three consecutive scans were used for data evaluation. The lipids were dissolved in highly purified water (2 mg/ml) and were kept above the phase transition for more than 1 h before measuring.

Neutrons

The sample used for in-plane neutron scattering was an equimolar mixture of DMPC/DSPC-d83, i.e., the higher melting component is perdeuterated. As a reference sample, we used an equimolar (protonated and chain-perdeuterated) mixture of one component: DMPC/DMPC-d54. Both samples were highly oriented phospholipid multilayers (stacks of ~3000 bilayers) on a polished quartz wafer (thickness 0.6 mm) with a mosaic spread of less than 4° and were prepared as described in detail previously (König et al., 1992). The water content of the multilayers was 25 wt-% D_2O, giving fully hydrated monolayers (Jürgens et al., 1983). For neutron scattering experiments, the sample was placed under a saturated D_2O atmosphere in a thermostated Aluminum sample holder with a temperature reproducibility of better than ±0.5°C.

The neutron scattering experiment was done at the EVA reflectodifractometer (Dosch et al., 1992) located at the ILL (Grenoble). Fig. 1 shows the setup of this instrument schematically. The angle of the incident beam with respect to the sample surface was $\alpha_i = 0.3°$, close to the critical angle α_c for total reflection. For low absorbing, nonmagnetic substances the critical angle α_c is given by (Russell, 1990)

$$\alpha_c = \sqrt{\frac{\lambda^2 N_A}{\pi} \sum_i \frac{\rho_i b_i}{A_i}}. \quad (1)$$

Here, λ is the neutron wave length, N_A is the Avogadro's number, and b_i is the neutron scattering length of component i with density ρ_i and atomic weight A_i. A position sensitive detector (PSD) at $2\theta = 0$ (i.e., in forward direction, cf. Fig. 1) detects three different contributions relevant for this experiment: 1) the specular reflection at $\alpha_f = \alpha_c$; 2) the transmitted signal at $\alpha_f \neq \alpha_c$, which is evanescent for $\alpha_f \leq \alpha_c$; and 3) the primary beam below the sample horizon at $\alpha_f = -\alpha_c$. Positioning the PSD out of the plane of incidence enables the measurement of neutrons undergoing evanescent scattering from structures in the sample surface with a correlation length l_c. The bulk signal from neutrons that enter and leave the sample via side edges and thus appear at $\alpha_f = -\alpha_c$ is screened by a cadmium slit.

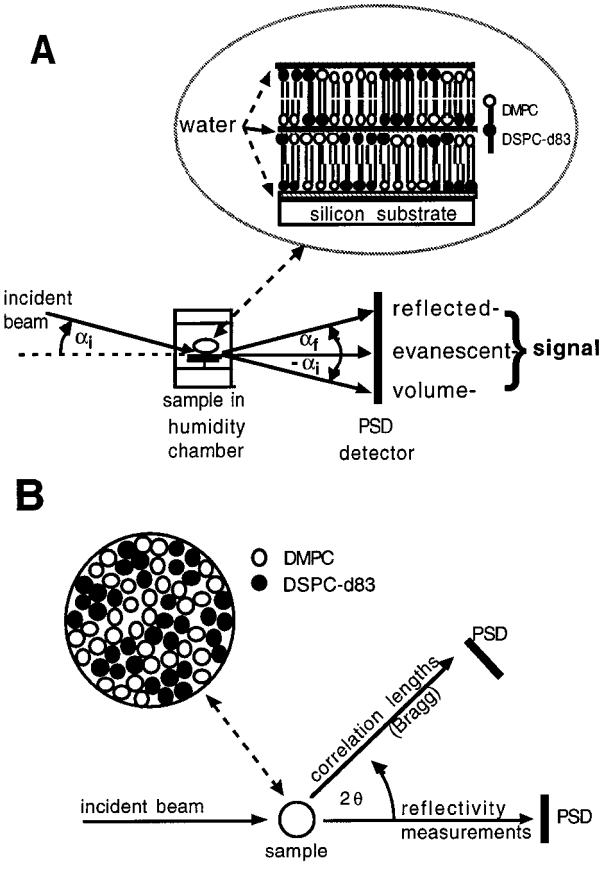

FIGURE 1 Experimental setup for measuring Bragg scattering of domains in oriented phospholipid multilayers. (*A*) Side view; (*B*) top view. Scattering contrast between domains and surrounding is achieved by using deuterated DSPC-d83, the situation of complete demixing of the two lipids as conveyed by the sketch represents an idealization.

As the bilayer planes of our multilayer sample are parallel to the surface, the only potential that can cause in-plane scattering is associated with the lateral distribution of domains within each bilayer, provided that there is a scattering contrast between the domain and its surroundings. This can be achieved by perdeuteration of the component that will get enriched in the domain. In our case, the high melting component DSPC is nearly fully deuterated except for the protons of the glycerol backbone (DSPC-d83). The minimum penetration depth d_s^{min} can be calculated approximately using $d_s^{min} = \lambda/(2\pi\alpha_c)$ (Dosch et al., 1992). A reflectivity measurement gives $\alpha_c = 0.3 \pm 0.1°$, independent of T between 10–55°C within the given error. This leads to a minimum scattering depth of ~170 Å, which is equivalent to about three bilayers.

The maximum scattering depth d_s^{max} was estimated by $= (Im\{Q_z'\})^{-1}$ (Dosch et al., 1986) where Q_z' is the momentum transfer in normal direction of the sample, which was calculated using lipid densities at full hydration (Knoll, 1981; Nagle and Wilkinson, 1978) and $\alpha_c = 0.3°$. This leads to a value of d_s^{max} that corresponds to ~80 bilayers.

For scatterers arranged in a two-dimensional lattice in a plane parallel to the surface (lattice constant expressed in terms of a coherence length l_c), the evanescent neutrons will be coherently scattered. Consequently, a diffraction peak can be observed (cf. Fig. 2) for angles Θ which satisfy the condition

$$l_c = \lambda/(2 \sin \theta). \quad (2)$$

Data acquisition was performed in 1024 channels of the PSD (10 channels/mm), covering a total ($\alpha_i + \alpha_f$) region from 0 to 2.7°. Binning of the channels into groups of 150 and using integral intensities from only those groups that cover angular regions where evanescent scattering is expected, gave very similar results but lower signal/noise ratio. This independence of domain scattering on the scattering depth is likely to be caused by the averaging over several bilayers (3–80 bilayers according to the above estimate) for all relevant scattering depths. Because interbilayer water decouples adjacent bilayers, the surface contribution to the scattering expected from the top bilayer of the multilayer stack (i.e., at the bilayer/air interface) is likely to become negligible as a result of the averaging.

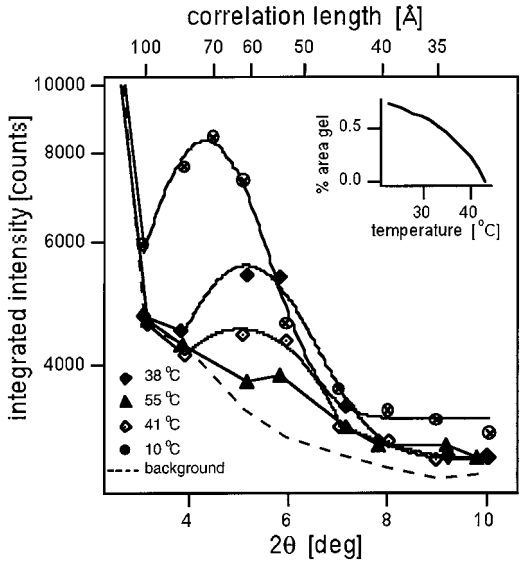

FIGURE 2 Neutron Bragg scattering under grazing angle of 1:1 DMPC/DSPC-d83 oriented multilayers at three temperatures corresponding to the fluid- (55°C), gel- (10°C), and coexistence- (38°C, 41°C) region of the mixture's phase diagram. The *inset* in the upper right corner shows the percentage of gel phase (domain) area (%-a_g) versus temperature in the coexistence region as calculated from the phase diagram (Knoll et al., 1981a) of this mixture.

AFM

The supported lipid bilayers for the AFM experiments were prepared from the vesicle phase: a suspension of small unilamellar vesicles was prepared at 65°C and incubated on freshly cleaved mica. The bilayers were then transferred to the AFM (Nanoscope III, Digital Instrument, Santa Barbara, CA.) and imaged in constant force mode in ultrapure water. Before imaging, the AFM was allowed to equilibrate for 60 min to minimize sample and cantilever drift. The cantilevers were commercial silicon nitride cantilevers (DNP-S TT, Digital Instruments, Santa Barbara, CA) with a nominal spring constant of 30 mN/m. Loading forces were kept below 200 pN, and scan rates varied from 2 Hz (lines per second) to 8 Hz. To minimize and correct for friction-induced height artifacts, the fast scan-axis was oriented perpendicular to the cantilevers axis of symmetry, and trace and retrace images were compared. All experiments were carried out at room temperature (25°C). The thickness of the single planar bilayer was determined at the sites of bilayer defects (holes in the bilayer that expose the bare mica) as 68 ± 2 Å and thus agrees well with x ray and neutron data (Büldt et al., 1978; Nagle and Wiener, 1988).

RESULTS

Neutron scattering

For our oriented multilayer sample, domains enriched in DSPC-d83 will dominate the coherent neutron scattering giving a signal at $\alpha_f \geq 0$. The scattering contrast is caused by the different degree of deuteration between the DSPC-d83 domains and the surrounding (nondeuterated) DMPC. The information obtained from the coherent scattering is related to how the domains with the DSPC-d83 are distributed in each bilayer plane and, in particular, to their average center to center distance l_c. Theory (Jorgensen et al., 1993; Lee, 1977) predicts the onset of DSPC-d83-enriched gel domain formation just below the liquidus temperature T_l (i.e., in the coexistence region of the DMPC/DSPC-d83 phase diagram). Consequently, no coherent scattering should occur for $T > T_l$. Furthermore, the existence of a crystal-like gel phase consisting of separated gel domains being either enriched or depleted in DSPC-d83 is predicted to occur just below the solidus temperature T_s. For our sample we have $T_l = 43°C$ and $T_s = 22°C$ and thus we can expect a coherent signal at $2\theta \neq 0$ (Fig. 1) arising from the domains for all $T < T_l$.

Fig. 2 shows the results of our EVA measurements (integral intensity vs. 2θ) obtained at four temperatures corresponding to the fluid ($T = 55°C$), the coexistence ($T = 38°C$ and $T = 41°C$), and to the gel ($T = 10°C$) phase of the bilayer. The integral intensity in Fig. 2 represents the sum over all 1024 channels for each value of 2θ. Beside the large specular peak for $2\theta \rightarrow 0$, we observe a second peak in the region $3° \leq 2\theta \leq 6°$ for all $T < T_l$ (i.e., at 41°C, 38°C, and 10°C) but not at $T = 55°C > T_l$. We found that this behavior was reversible and independent of whether the measurement was performed under conditions of increasing or decreasing temperature.

Strong evidence that coherent scattering from domains is indeed the origin of the peak observed, for all $T < T_l$ comes from the DMPC/DMPC-d52 control sample (Fig. 3). For this mixture we have $T_l = 19.6°C$ and $T_s = 19.2°C$ (Bayerl

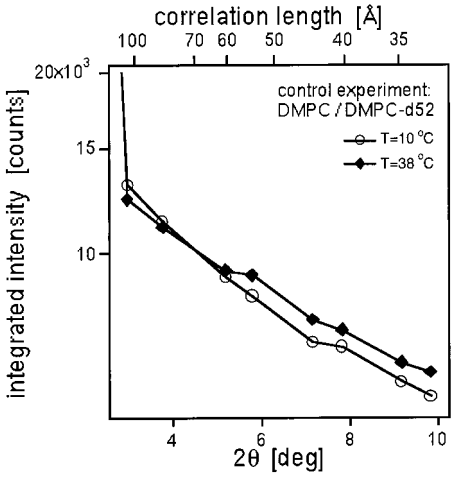

FIGURE 3 Neutron Bragg scattering under grazing angle of 1:1 DMPC/DMPC-d54 oriented multilayers at two temperatures corresponding to the fluid (38°C) and to the gel phase (10°C) of this mixture.

et al., 1988), and no domain formation is expected at any temperature because of its nearly ideal mixing behavior. Indeed, a measurement at $T = 10$°C, which is in the gel phase well below T_s, gives no peak in the region $3° \leq 2\theta \leq 6°$, and the result is similar to that obtained at $T = 38$°C $> T_l$ (fluid phase), indicating a homogeneous distribution of protonated and deuterated DMPC in both phase states. This strongly suggests that the peak observed for DMPC/DSPC-d83 for all $T < T_l$ was caused by a heterogeneous distribution of both lipids, i.e., by the domains.

For the peaks measured for DMPC/DSPC-d83 at $T < T_l$, we can use eq. 2 to calculate the coherence length l_c between the domains. The results are listed in Table 1 for the limiting values of the peaks shown in Fig. 2 ($2\theta^{min}$, $2\theta^{max}$ giving l_c^{min} and l_c^{max}) and for the peak center position (giving l_c^{av}). We interpret the coherence length l_c^{av} as the average center to center distance between two adjacent domains.

Atomic force microscopy

The AFM used in our study was restricted to room temperature use only. For this reason, it was not appropriate for studying the DMPC/DSPC-d83 mixture whose solidus line is at $T_s = 22$°C. We found the AFM results obtained under such conditions ($T \leq T_s$) are ambiguous because of the restricted mechanical stability of the bilayer for temperatures in the vicinity of T_s. Therefore, we used a binary mixture of DPPC/DAPC (1:1) having a more elevated value of $T_s = 42$°C for the AFM experiments. This mixture exhibits the same chain mismatch (four methylene groups) as the DMPC/DSPC mixture, but the fatty acyl chains of each component is longer by two methylene groups. Consequently, the phase diagram of this mixture is very similar to that of DMPC/DSPC when compared at reduced temperatures (Fig. 4). We assume that the results obtained with this mixture are indicative of those expected for DMPC/DSPC at the same reduced temperature.

Fig. 5 *A* and *B* shows AFM data obtained at temperatures well below T_s in the gel phase of the equimolar DPPC/DAPC mixture at different magnifications. Geometrically not well defined but clearly separated plateau regions of essentially two different heights are observed with average lateral extensions (real space diameter) ranging from 4–60 nm. The height difference between the regions is 0.4 ± 0.1 nm. This is very close to the theoretical all-trans-length difference of 0.5 nm between the two lipid components. Furthermore, both regions occupy roughly the same area. These findings indicate that the two regions correspond to a mixture of gel phase domains either enriched in DAPC and depleted in DPPC and vice versa. A control sample of pure DAPC at the same temperature shows a completely different and much smoother height scan structure (Fig. 5 *C*). The maximum height difference observed here over distances comparable with those studied for the mixture was only 0.1–0.2 nm, and no plateau regions characteristic of domains were observed. Nevertheless, pure DAPC gel phase

TABLE 1 Minimum, maximum and average coherence length l_c between the domains of DMPC/DSPC-d83 calculated from the neutron data in Fig. 2 for the gel phase (10°C) and the coexistence region (38 and 41°C)

Method	Temperature (°C)	Phase state	l_c^{min} (nm)	l_c^{max} (nm)	l_c^{av} (nm)
Neutron	10	Gel	6.2	9.1	7.4
Neutron	38	Coexistence	5.1	7.5	6.0
Neutron	41	Coexistence	5.3	7.8	6.3
AFM	25	Gel	4.0	50.0	10.1

For comparison, the domain distances obtained by the Fourier-transformed AFM data of gel phase DPPC/DAPC are given. The error of the neutron data was estimated as ±0.5 nm on the basis of the residual mean square deviation of fitting the peaks in Fig. 2 to gaussians. For AFM, the error is ±2 nm (l_c^{min} and l_c^{av}) and ±20 nm for l_c^{max}.

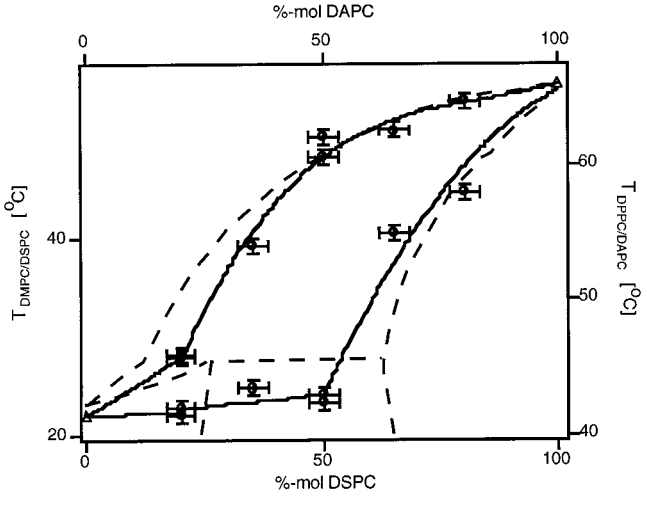

FIGURE 4 Comparison of the phase diagram of DMPC/DSPC (*dashed line*) taken from (Knoll et al., 1981a) with that determined by DSC for DPPC/DAPC (*open circles*). Note the offset in the temperature axis for both mixtures. The *full line* represents a fit to the DSC data to facilitate the comparison.

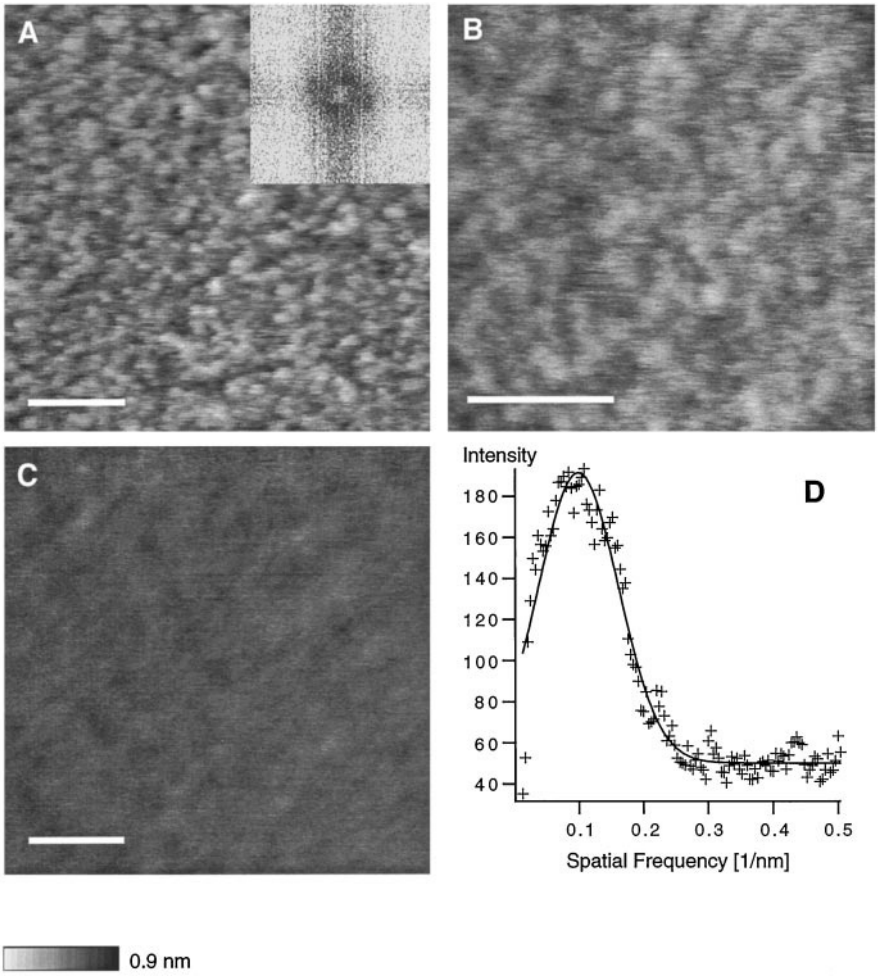

FIGURE 5 (*A*) AFM micrograph of a 1:1 DPPC/DAPC bilayer on a solid support (mica) at 25°C (gel phase) and its two-dimensional Fourier transform (*right insert*). (*B*) High resolution image of the same bilayer as in *A*. (*C*) AFM micrograph of a DAPC bilayer on a solid support (mica) at 25°C (gel phase) with the gray scales height encoding identical to that in Fig. 5, *A* and *B*. Imaging parameters for *A* to *C*: raw data baseline corrected, constant force (≤0.2 nN), silicon-nitride-tip (30 mN/m), 1.8 μm/s (*A*), 0.8 μm/s (*B*), 1.3 μm/s (*C*) scan speed. The z-range extends from 0.0 nm (*black*) to 0.9 nm (*white*) for all three images. Scale bars, 50 nm. (*D*) The average radial intensity of the two-dimensional Fourier transform of Fig. 5 *A*. A gaussian distribution (*full line*) can be fitted to the data (*crosses*) to compare it with neutron scattering results.

surfaces seem to exhibit a certain wave-like character. It may arise from the formation of the gel phase of a pure lipid under lateral tension because of the presence of the mica solid support. It has been demonstrated that under such conditions the formation of a ripple structure ($P_{\beta'}$-phase) is prevented (Johnson et al., 1991) in favor of a less wavy $P_{\beta*}$ phase.

The regular spacing of the domain pattern of the DPPC/DAPC mixtures can be expressed quantitatively by the two-dimensional Fourier transform of the AFM data, which is shown in Fig. 5 *A* (*insert*). However, one has to keep in mind that the AFM does not directly visualize the two different components of the bilayer but only the resulting surface topography. As mentioned above, even pure DAPC bilayers show some height variation, particularly in the low frequency regime. Consequently, this background height variation of a single lipid component will be superimposed with the height signal caused by lipid demixing in the topographic image of the DPPC/DAPC mixture. In contrast, neutrons get in-plane diffracted at the regions of highest scattering contrast gradients established by the demixing caused by the isotopic substitution of one lipid component and do not show any coherent signals for ideal mixing samples (Fig. 3). Thus, in order to account for the topographic contribution of the single component AFM data to those of the binary sample for comparison with the neutron results, we subtracted the Fourier transform of the single component AFM control experiment from that of the mixed system. This approach gave the Fourier transforms shown in Fig. 5, *A* and *D*. The circular pattern in the two-dimensional Fourier transform at 0.099 nm^{-1} corresponding to a wavelength of 10.1 ± 2 nm (Fig. 5 *A*) clearly reflects the regular spacing and the isotropic distribution of the domains in the bilayer. A one-dimensional cross section of this two-dimensional Fourier transform as shown in Fig. 5 *D* allows now a direct comparison between AFM and neutron scattering data. Because of the limited lateral extension of the bilayer covered by the AFM, the low frequency limit of the distribution can only be estimated as ~0.02 nm^{-1}, corresponding to a wavelength of 50 nm. On the other side, the high frequency cut-off is at 0.254 nm^{-1} (inflection point of the fitted gaussian), corresponding to a wavelength of 3.94 nm.

DISCUSSION

The gel phase ($T < T_s$) AFM results obtained for a DPPC/DAPC mixture of a very similar phase behavior to that of

DMPC/DSPC provide evidence that the average domain size is ~10 nm. This result of unsurpassed directness in domain detection can now be compared with the gel phase neutron results. Although the neutrons are the less direct technique and the results expressed in terms of reciprocal rather than real space, they offer one major advantage over the AFM. This is the fact that the neutrons can also probe the sample in the coexistence and in the fluid phase where the nonnegligible contact interaction force between AFM tip and lipid surface may alter the object under study or may prevent its detection at all. To appreciate the neutron results in terms of a domain size, we have to distinguish between 1) the case of two immiscible gel domains (denoted as gel-1 and gel-2 in Knoll et al., 1981a) for $T < T_s$ and 2) the case of a DSPC-d83 enriched gel domain embedded in a fluid phase for $T_s < T < T_l$.

Case 1: From the similarity of the molecular area of DMPC and DSPC and from consideration of the phase diagram of this mixture we can assume that gel-1 and gel-2 domains each occupy roughly 50% of the total bilayer area. This is supported by FT-IR results (Brumm et al., 1996). Assuming hexagonal packing of circularly shaped gel domains (diameter d_g), we can estimate a maximum value for $d_g = 2l_c^{av}/3 = 50$ Å. Case 2: Here the domain diameter d_f is $d_f \leq d_g \leq l_c^{av}$.

Hence, the upper limit of l_c at $T < T_s$ (gel phase) as estimated from the neutron results is smaller than that obtained by the AFM Fourier transform, most likely owing to the limited total bilayer area covered by the AFM measurement. In contrast, the lower limits and the average coherence length agree well for both methods (Table 1). We conclude that the Fourier transform of the AFM data is indeed the most suitable base for a comparison with the neutron results. However, as the AFM clearly shows that the gel domains are not circular but of a rather complex shape, our estimates for d_g (case 1) fall inevitably short compared with the AFM (real space) domain diameters. Furthermore, there is a number of other intrinsic methodological differences that may require consideration. One is that the boundaries in scattering contrast between domains and their surroundings, as seen by the neutrons, may not coincide exactly with the plateau boundaries detected by AFM. Moreover, our data analysis in terms of eq. 2 assumes point scatterers in a lattice and does not consider their spatial extension. Furthermore, there might be some broadening of the plateau edges seen by AFM because of the shape and the lateral extension of the AFM tip. Finally, there might still be some difference in the size of the domains for the two binary mixtures studied by either method despite the similarity of their phase diagrams.

Nevertheless, we conclude that AFM and neutrons provide complementary data on domain size and periodicity that agree very well, considering the differences in the fundamental character of the two types of measurement. This gives us the required confidence to consider the neutron data for the coexistence region as truly reflecting the correlation distances between gel phase domains embedded in a fluid.

From the *insert* in Fig. 2, we obtain a gel domain contribution to the total bilayer area of 19 and 30% at 41 and 38°C, respectively, as determined from the phase diagram (Knoll et al., 1981a) and the known molecular area of the lipids in both phase states (Nagle and Wiener, 1988). However, despite this considerable change of total gel area, l_c^{av}, and thus the domain spacing is similar at both temperatures (Table 1). On the other hand, the intensity difference between the peaks at 41 and 38°C agrees well with the 11% change of gel phase area between the two temperatures. For this estimate, the intensity obtained at 10°C was assumed to represent 100% gel phase area. This indicates that domain spacing did not change significantly upon increase of the total gel phase area. Hence, individual domains do not grow at the expense of the fluid between them but rather an increase in gel area is established via the formation of new gel domains out of the bulk fluid. As a result, a superstructure consisting of equally spaced domains of size d_f surrounded by a constant amount of fluid phase may be formed (Fig. 6) until the interdomain fluid freezes out at $T \leq T_s$, leading to a mixture of gel-1 and gel-2 domains as seen by the AFM. The interdomain fluid may explain why fluorescence (Almeida et al., 1992) and spin label methods (Sankaram et al., 1992) observe a disconnection (percolation) for this mixture in the coexistence region that is not observed by NMR methods (Dolainsky et al., 1997). For geometrical reasons, the bulky fluorescence and spin labels may be enriched in the fluid bulk phase between the superstructures but depleted in the fluid separating the domains. In contrast, the label-free NMR methods sample the average mobility of all fluid molecules over a shorter experimental length scale, thus detecting diffusion even under conditions when the bulk fluid becomes disconnected by the growth of the superstructures (Fig. 6 *D*).

It is interesting to compare our results for domain spacing with those values obtained by far less direct methods. A center to center distance of 19–23 nm was concluded from an ESR study of this mixture at 40°C (Sankaram et al., 1992), whereas a domain size of $d \approx 80$ nm was suggested from fluorescence experiments (Almeida et al., 1992). Both studies were done at temperatures T in which $T_s < T < T_l$, and they invoked a number of model assumptions for the estimation of these values. Moreover, both relied on the measurement of a dynamical parameter like the diffusion coefficient and thus were associated with a certain characteristic time and length scale. In contrast, our neutron experiment averaged over very long measuring times compared with all types of motions in the bilayer. This difference may explain why our neutron results give smaller or, in the case of fluorescence experiments, substantially smaller l_c values in the coexistence region. No values for l_c below T_s have been reported for DMPC/DSPC, but an infrared study of a (4:1) C_{18}/C_{22} lecithin mixture (i.e., same chain length mismatch as in our sample) suggests domain sizes of the minority (high melting) component of ~20 Å in

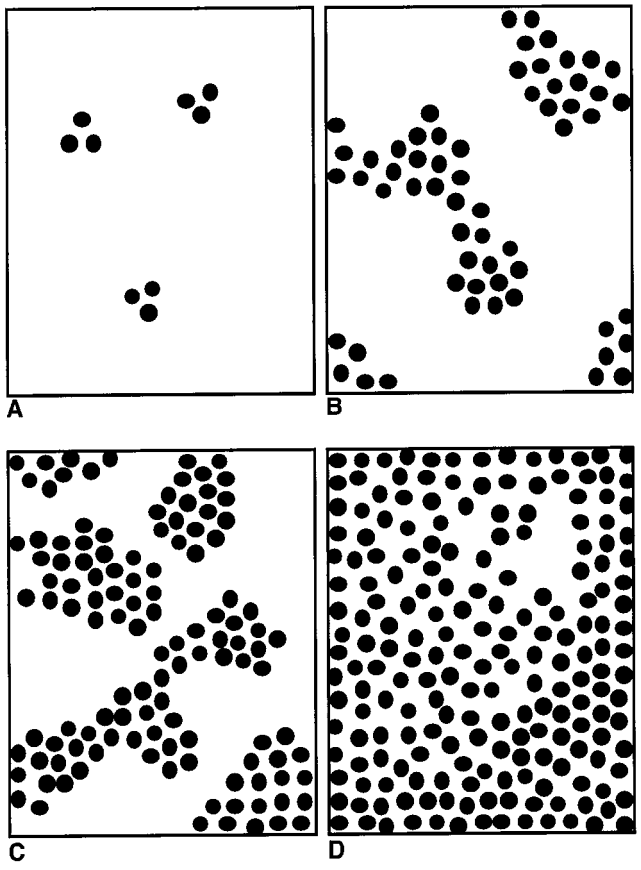

FIGURE 6 Schematic depiction of the growth of superstructures consisting of equally spaced gel domains (assumed circular in shape) with decreasing temperature within the coexistence region of the phase diagram. After the initial formation of very few gel domains just below T_1 (*A*) their number increases in accordance with the increase in the total gel phase area (*B* and *C* show the situation at 19 and 30% gel phase) until all bulk fluid is gone and the fluid spaces between the gel domains freeze out at T_s (*D*).

the solid phase (Mendelsohn et al., 1995). This is close to our results for $T < T_s$, taking into account that we used a 1:1 mixture.

CONCLUSION

We have shown using two independent, complementary and direct methods that domains in lipid bilayers are three orders of magnitude smaller than those observed in lipid monolayers. The good agreement between AFM and neutron results despite the completely different nature of their observables (AFM sees real space whereas neutron scattering is sensitive to reciprocal space) can help in the development of refined models for the neutron data interpretation in terms of regularly spaced and spatially extended scatterers.

We thank Professor Hermann Gaub, in whose laboratory the AFM measurements were conducted, for support and helpful discussions.

REFERENCES

Almeida, P. F. F., W. L. C. Vaz, and T. E. Thompson. 1992. Lateral diffusion and percolation in two-phase–two-component lipid bilayers: topology of the solid-phase domains in-plane and across the lipid bilayer. *Biochemistry* 31:7198–7210.

Bayerl, T. M., C. F. Schmidt, and E. Sackmann. 1988. Kinetics of symmetric and asymmetric phospholipid transfer between small sonicated vesicles studied by high-sensitivity differential scanning calorimetry, NMR, electron microscopy, and dynamic light scattering. *Biochemistry* 27:6078–6085.

Brumm, T., K. Jorgensen, O. G. Mouritsen, and T. M. Bayerl. 1996. The effect of increasing membrane curvature on the phase transition and mixing behavior of a dimyristoyl-sn-glycero-3-phosphatidylcholine/distearoyl-sn-glycero-3-phosphatidylcholine lipid mixture as studied by Fourier transform infrared spectroscopy and differential scanning calorimetry. *Biophys. J.* 70:1373–1379.

Büldt, G., H. U. Galley, A. Seelig, J. Seelig, and G. Zacci. 1978. Neutron diffraction studies on selectively deuterated phospholipid bilayers. *Nature.* 271:182–184.

Dolainsky, C., P. Karakatsanis, and T. M. Bayerl. 1997. Lipid domains as obstacles for lateral diffusion in supported bilayers probed at different time and length scales by two-dimensional exchange and field gradient solid state NMR. *Phys. Rev. E.* 55:4512–4521.

Dosch, H., K. AlUsta, A. Lied, W. Drexel, and J. Peisl. 1992. The evanescent neutron wave diffractometer: on the way to surface sensitive neutron scattering. *Rev. Sci. Instrum.* 63:5533–5542.

Dosch, H., W. Battermann, and D. C. Wack. 1986. Depth-controlled grazing-incidence diffraction of synchrotron X radiation. *Phys. Rev. Lett.* 11:1144–1148.

Dufrêne, Y. F., W. R. Barger, J. D. Green, and G. U. Lee. 1997. Nanometer-scale surface properties of mixed phospholipid monolayers and bilayers. *Langmuir.* 13:4779–4784.

Groves, J. T., N. Ulman, and S. G. Boxer. 1997. Micropatterning fluid lipid bilayers on solid supports. *Science.* 275:651–653.

Hansma, P. K., J. P. Cleveland, M. Radmacher, D. A. Walters, P. E. Hillner, M. Bezanilla, M. Fritz, D. Vie, H. G. Hansma, C. B. Prater, J. Massie, L. Fukunaga, J. Gurley, and V. Elings. 1994. Tapping mode atomic force microscopy in liquids. *Appl. Phys. Lett.* 64:1738–1740.

He, K., S. J. Ludtke, D. L. Worcester, and H. W. Huang. 1996. Neutron scattering in the plane of membranes: structure of alamethicin pores. *Biophys. J.* 70:2659–2666.

Johnson, S. J., T. M. Bayerl, D. C. McDermott, G. W. Adam, A. R. Rennie, R. K. Thomas, and E. Sackmann. 1991. Structure of an adsorbed dimyristoylphosphatidylcholine bilayer measured with specular reflection of neutrons. *Biophys. J.* 59:289–294.

Jorgensen, K., M. M. Sperotto, O. G. Mouritsen, J. H. Ipsen, and M. J. Zuckermann. 1993. Phase equilibria and local structure in binary lipid bilayers. *Biochim. Biophys. Acta.* 1152:135–145.

Jürgens, E., G. Höhne, and E. Sackmann. 1983. Calorimetric study of the dipalmitoylphosphatidylcholin/water phasediagram. *Ber. Bunsenges. Phys. Chem.* 87:95–104.

Knoll, W. 1981. Volume determination of deuterated dimyristoyllecithin by mass and scattering length densiometry. *Chem. Phys. Lipids.* 28: 337–345.

Knoll, W., J. Haas, H. B. Stuhrmann, H. H. Füldner, H. Vogel, and E. Sackmann. 1981a. SANS of aqueous dispersions of lipids and lipid mixtures: a contrast variation study. *J. Appl. Cryst.* 14:191–202.

Knoll, W., K. Ibel, and E. Sackmann. 1981b. SANS study of lipid phase diagrams by the contrast variation method. *Biochemistry.* 20: 6379–6383.

Knoll, W., G. Schmidt, H. Rotzer, T. Henkel, W. Pfeiffer, E. Sackmann, S. Mittlerneher, and J. Spinke. 1991. Lateral order in binary lipid alloys and its coupling to membrane functions. *Chem. Phys. Lipids.* 57:363–374.

Knoll, W., G. Schmidt, E. Sackmann, and K. Ibel. 1983. Critical demixing in fluid bilayers of phospholipid mixtures: a neutron diffraction study. *J. Chem. Phys.* 79:3439–3442.

König, S., W. Pfeiffer, T. Bayerl, D. Richter, and E. Sackmann. 1992. Molecular dynamics of lipid bilayers studied by incoherent quasi-elastic neutron scattering. *J. Phys. II France.* 2:1589–1615.

Lee, A. G. 1977. Lipid phase transitions and phase diagrams. *Biochim. Biophys. Acta.* 472:237–344.

Lee, A. G. 1978. Calculation of phase diagrams for non ideal mixtures of lipids—and a possible non random distribution of lipids in lipid mixtures in the liquid crystalline phase. *Biochim. Biophys. Acta.* 507:433–444.

Loidl-Stahlhofen, A., S. Kaufmann, T. Braunschweig, and T. M. Bayerl. 1996. The thermodynamic control of protein binding to lipid bilayers for protein chromatography. *Nature Biotechnol.* 14:999–1002.

Lösche, M., E. Sackmann, and H. Möhwald. 1983. Fluorescence microscopic study concerning the phase diagram of phospholipids. *Ber. Bunsenges. Phys. Chem.* 87:848–852.

McConnell, H. M. 1991. Structures and transitions in lipid monolayers at the air-water interface. *Annu. Rev. Chem. Phys.* 42:171–195.

McConnell, H. M., L. K. Tamm, and R. M. Weis. 1984. Periodic structures in lipid monolayer transitions. *Proc. Natl. Acad. Sci. USA.* 81: 3249–3253.

Mendelsohn, R., G. L. Liang, H. L. Strauss, and R. G. Snyder. 1995. IR spectroscopic determination of gel state miscibility in long-chain phosphatidylcholine mixtures. *Biophys. J.* 69:1987–1998.

Möhwald, H. 1990. Phospholipid and phospholipid-protein monolayers at the air/water interface. *Annu. Rev. Chem. Phys.* 41:441–476.

Mouritsen, O. G. 1991. Theoretical models of phospholipid phase transitions. *Chem. Phys. Lipids.* 57:179–194.

Nagle, J. F. and M. C. Wiener. 1988. Structure of fully hydrated bilayer dispersions. *Biochim. Biophys. Acta.* 942:1–10.

Nagle, J. F. and D. A. Wilkinson. 1978. Lecithin bilayers. *Biophys. J.* 19:159–175.

Pedersen, S., K. Jorgensen, T. R. Baekmark, and O. G. Mouritsen. 1996. Indirect evidence for lipid-domain formation in the transition region of phospholipid bilayers by two-probe fluorescence energy transfer. *Biophys. J.* 71:554–560.

Rädler, J., M. Radmacher, and H. E. Gaub. 1994. Velocity dependent forces in atomic force microscopy imaging of lipid films. *Langmuir.* 11:3111–3115.

Radmacher, M., M. Fritz, H. G. Hansma, and P. K. Hansma. 1994. Direct observation of enzyme activity with the atomic force microscope. *Science.* 265:1577–1579.

Russell, T. P. 1990. X-ray and neutron reflectivity for the investigation of polymers. *Mat. Sci. Rep.* 5:173–271.

Sankaram, M. B., D. Marsh, and T. E. Thompson. 1992. Determination of fluid and gel domain sizes in two component, two-phase lipid bilayers: an electron spin resonance spin label study. *Biophys. J.* 63:340–349.

Shao, Z. and J. Yang. 1995. Progress in high resolution atomic force microscopy in biology. *Q. Rev. Biophys.* 28:195–251.

Tate, M. W., E. F. Eikenberry, D. C. Turner, E. Shyamsunder, and S. M. Gruner. 1991. Nonbilayer Phases of Membrane Lipids. *Chem. Phys. Lipids.* 57:147–164.